A LARGE STEPWISE MOTION ELECTROSTATIC ACTUATOR FOR A WIRELESS MICROROBOT

P. Basset, A. Kaiser, P. Bigotte, D. Collard* and Lionel Buchaillot

IEMN Dpt ISEN (Villeneuve d'Ascq, FRANCE) - UMR CNRS 8520
*CIRMM / IIS-The University of Tokyo
Phone: (+33) 3 20 19 78 38, Fax: (+33) 3 20 19 78 84, E-mail: philippe.basset@isen.fr

ABSTRACT

An original large stepwise motion electrostatic microactuator for a wireless microrobot using a distributed Ciliary Motion System (CMS) [1] is presented. Coventorware™ cosolver simulations have shown x-displacement of 240 nm for one actuation step. Design of the antennas for inductive powering has been optimized in order to maximize the energy transfer. 24 µm gold electroplated hollow micro-coils have been fabricated on an epoxy substrate as receiver antennas. Q-factor of 29 at 13.56 MHz and induced voltage up to 100 V on a 1 kΩ load has been obtained. Remote actuation of an array of actuators supporting a 0.25 mm^2/380 µm-thick piece of silicon has been successfully demonstrated with a pull-in voltage of 80 V.

INTRODUCTION

The realization of a completely autonomous microrobot is a significant challenge for the future. Many applications are expected, particularly in the field of the micro assembly and the test of various devices in confined environment [2]. A typical walking microrobot was realized thanks to the use of polyimide joints thermally actuated [3]. However, the need of a very significant power makes difficult its remote powering. An overview of the system we propose is shown in figure 1. Electrostatic actuation seems to be a better candidate since only a few mW are required to generate strong forces [4]. In addition to the achievement of the actuator itself, two major difficulties have to be overcome while designing a wireless microrobot. First, the emitter/receiver coupling has to be optimized while minimizing the losses of transmitted power. Second, all the components needed for the power reception and the control of the robot must be as light as possible. As a concequence, the conductor resistivity must be minimized to obtain a high quality factor. The use of an insulating substrate prevents the losses due to Eddy currents from occurring and reduces the substrate parasitic capacitance. Concerning the weight that the robot will have to support, it is strongly decreased thanks to the realization of the antenna on an epoxy film, which will be separate from the wafer in order to be hybridized upon the microrobot.

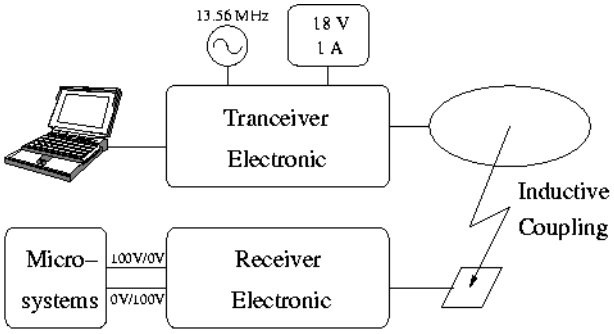

Figure 1: 0verview of the system.

ACTUATOR PART

The actuator (fig. 2) is build from self assembling polysilicon process [5] with an additional level of polysilicon. It is composed of a clamped-free plate partially covering a buried electrode. The applied voltage on the buried electrode enables the pull-in of the moving part towards the substrate due to electrostatic forces. When the stopper contacts the substrate, an axis of torsion is created which induces the rise of the plate free-end, with x and z displacements. An elevator is added to compensate the gap between the stopper and the substrate.
The dimensions of the capacitive part is 60*75 $µm^2$, and the distance between the stopper and the elevator position is 30 µm. The gap between the mobile plate and the buried electrode is 1.4 µm and height of the stopper is 1µm. Coventorware™ cosolver simulations, with a 1 µm-thick

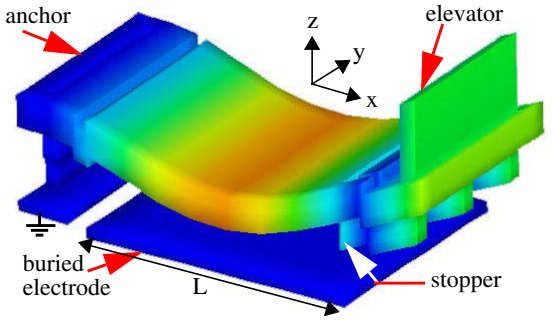

Figure 2: Actuator view from Coventorware™ visualizer with *10 magnitude in the z-axis.

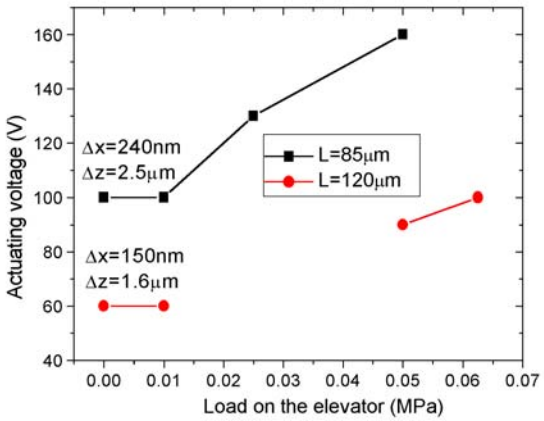

Figure 3: Actuating voltage as a function of the mechanical load applied on the elevator whose suface is 600 μm^2, for a 1μm-thick actuator. Coventorware™ cosolver simulation.

mobile part, have shown an x and z displacement respectively of 240 nm and 2.5 μm (fig. 3). An array of actuators is shown in figure 4.

ANTENNA PART

Fabrication

The process flow of the antenna fabrication is shown in figure 5. First, 2 μm Low Temperature Oxide (LTO) was deposited on a silicon wafer as sacrificial layer. Then, 150 μm of epoxy-type resist SU-8 is spun up. This film, once polymerized, will become a flexible, tough and light substrate. The conductor is made of thick electroplated gold. So a thin layer of nickel is sputtered in order to make the substrate conductive and to allow the electrolysis to be achieved. A 30 μm thick mold of positive resist AZ 4562 is realized and followed by gold plating. Finally the mold is removed, the seed layer of nickel is etched by nitric acid

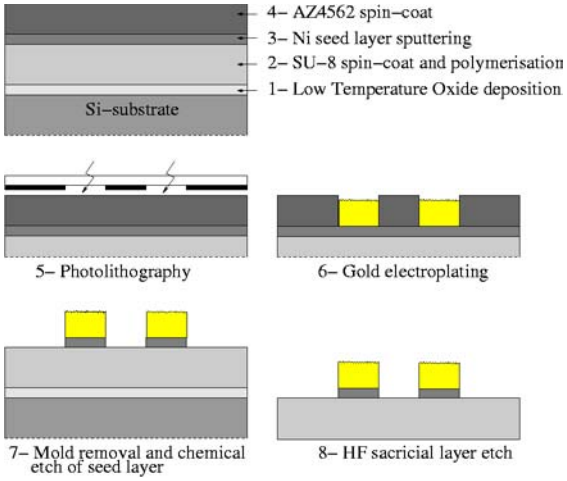

Figure 5: Process flow of the receiver antenna.

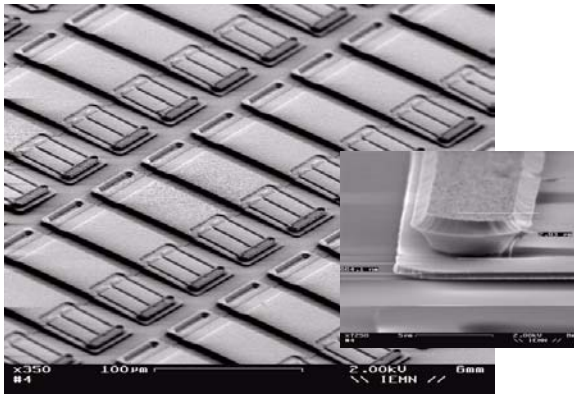

Figure 4: SEM picture of an array of actuators with close view of the elevator.

and the SU-8 film is separated from the silicon using hydrofluoric acid. Three hollow coil antennas with different designs have been fabricated (fig. 6). The outer diameter d_o of the coils is 15 mm and the space between the gold turns is 100 μm. The turn number of antennas #1, 2 and 3 are respectively 16, 26 and 23, and the conductor widths are 62.5 μm, 100 μm and 100 μm.

Measurement and Q-factor extraction

Antennas testing was performed with an Agilent 8753ES Network Analyzer. One-port S parameters were measured from 30 KHz to 100 MHz and converted to impedance Z_L. Then the parasitic capacitance *Cp* of the test device was de-embedded using open calibration of the device. Parameter extraction is deduced from an equivalent circuit consisting of a capacitor *C* in parallel with an inductance *L* in series with a resistor *R*. To extract *L* and *C* some assumptions need to be made.

As frequency increases, the penetration of the magnetic field into the conductor is attenuated (skin effect), which causes a reduction in the magnetic flux internal to the conductor. However *L* does not decrease significantly with increasing frequency because it is predominantly determined by the magnetic flux external to the conductor

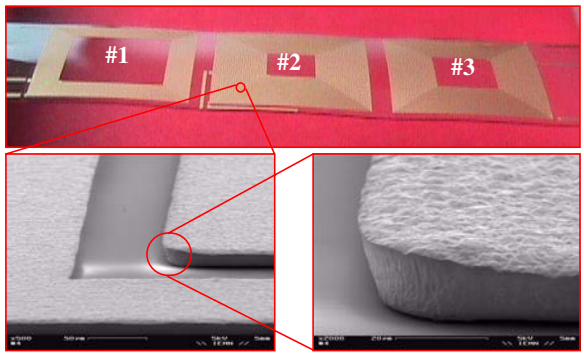

Figure 6: Overview and close SEM pictures of 24 μm-thick gold electroplated coils on SU-8 film.

Table 1: Characteristics of receiver antennas.

	Antenna 1	Antenna 2	Antenna 3
L (µH)	5.8	7.8	7.2
Self Resonance Frequency (MHz)	54	49	62
C (pF)	1.5	1.3	0.92
Q_L (13.56 MHz)	19	27	29
Q_L max	27 (27MHz)	32 (15.5MHz)	37 (19MHz)

[6]. Thus L can be approximated as constant with frequency. C is considered independent of frequency since it represents the metal-to-metal overlap capacitance between the turns. L is extracted from low-frequency imaginary part of Z_L and C is extracted using the low-frequency L value and the resonance frequency of the antenna. The quality factor Q_L is estimated by taking the ratio of the imaginary and real parts of the one-port impedance, observing Z_L is purely inductive in the frequency range of interest. Results are summed up in table 1.

ENERGY TRANSFER OPTIMIZATION

Receiver micro coil optimization

For the circuit in figure 8, the relationship between the induced voltage u_2 and the magnetic coupling of antennas, for a sinusoidal alternating current i_1 and the receiver antenna tuned with the emitter frequency ω_0 (in the non complex form) [7] is given by:

$$u_2 = \frac{\omega_0 \cdot k\sqrt{L_1 L_2}}{\sqrt{\left(\frac{r_2}{R_L}\right)^2 + \omega_0^2 \cdot \left(C_2 \cdot r_2 + \frac{L_2}{R_L}\right)^2}} \cdot i_1 \qquad (1)$$

where k is the coupling factor between antennas, r_2 the serial losses of L_2, and $\omega_0 = 1/(L_2.C_2)^{1/2}$

The simplest way to get the transmitter antenna is to use a circular electrical wire which the inductive value is given by:

$$L_1 = n_1^2 \cdot \mu_0 \cdot r_{a1} \cdot \ln\left(\frac{2 \cdot r_{a1}}{e_1}\right) \text{ for } r_{a1} >> e_1 \qquad (2)$$

where n_1 is the number of loops, r_{a1} the radius of loop, and e_1 the wire diameter.

For a given area, the best shape to maximize the coupling

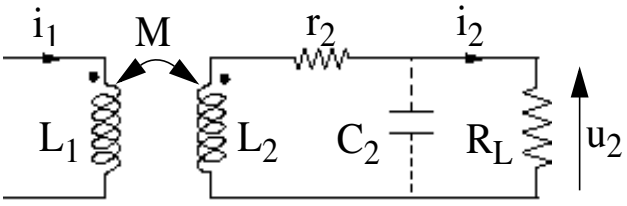

Figure 8: Electrical model of antennas.

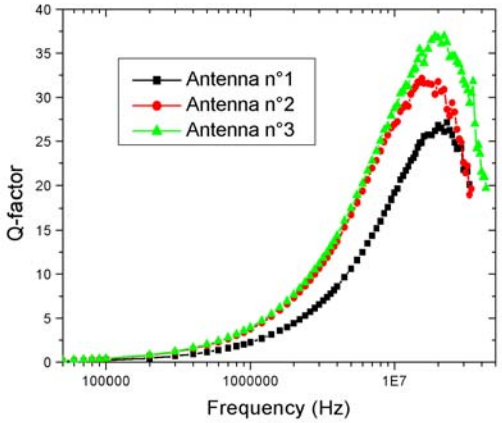

Figure 7: Q-factor of receiver antennas.

factor is obtained with a square coil as receiver antenna. As inner turns increase serial losses without having a high contribution to the inductance, a "hollow" coil should be used. Its value can be written as [8]:

$$L_2 \approx \frac{45 \cdot \mu_0 \cdot n_2^2 \cdot r_{a2}^2}{11 \cdot d_0 - 14 \cdot r_{a2}}; \qquad r_{a2} = \frac{d_0 + d_i}{4} \qquad (3)$$

where n_2 is the number of turns, d_0 the diameter of the coil, d_i its internal diameter, and r_{a2} the mean radius of the coil. Considering a constant magnetic field through the receiver antenna, the coupling factor can be approximated by:

$$k \approx \frac{4}{\pi} \cdot \frac{r_{a1}^2 \cdot r_{a2}^2}{\sqrt{r_{a1} \cdot r_{a2}} \cdot \sqrt{d^2 + r_{a1}^2}^3} \qquad (4)$$

where d is the distance between antennas.

The AC resistance of the coil due to the skin effect is given by:

$$r_2 \approx \frac{8 \cdot n_2 \cdot r_{a2}}{\sigma \cdot \delta \cdot (1 - e^{-t/\delta}) \cdot w}; \qquad \delta = \frac{1}{\sqrt{\pi \cdot f \cdot \mu_0 \cdot \sigma}} \qquad (5)$$

where σ is the conductivity of the conductor, t its thickness, w its width, and δ the skin depth.

According to these equations, induced voltage simulations show an optimum turn number for given hollow-coil area

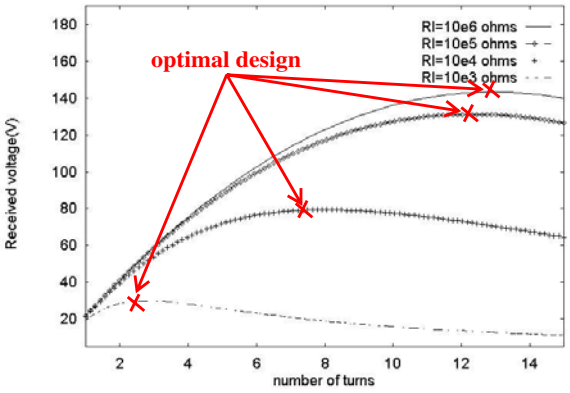

Figure 9: Simulation of induced voltage for a given hollow coil versus the loop number of identically spaced whorls.

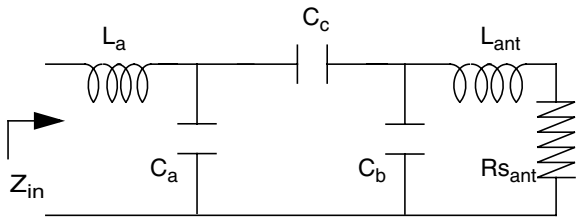

Figure 10: Schematic of the impedance matching circuit.

and load value (figure 9). This optimum, corresponding to the highest value of the inductance while keeping its serial losses at minimum, depends of the consumed current. Indeed, the more the load decreases, the more the influence of the electrical resistance of L_2 is prevalent. For an infinite load, the optimum turn number corresponds to a whorl width equivalent to the space between them.

Impedance matching of transmitter antenna

Dimensions of the transmitter antenna has also a serious effect on the induced power. Reducing its diameter increases the received voltage but only for small distances, since the coupling factor k is then closer to 1. Another important point to consider is the impedance matching between the antenna and the electrical circuit which has to provide the modulated AC current i_1. The L-C network proposed in figure 10, called T-match [8], allows all kinds of impedance matching. Having symmetrical components as L_a=L_{ant} and C_a=C_b guarantees Z_{in} is purely resistive. The presence of C_c permits to win one degree of freedom and to state independent equations of C_a and C_c, depending of Rs_{ant}, Z_{in} and ω_o.

$$C_a = C_{eq} \cdot \frac{1}{1 + \sqrt{\frac{Z_o \cdot Rs_{ant} \cdot C_{eq}}{L_{ant}}}} \quad (6)$$

$$C_1 = C_{eq} \cdot \frac{\sqrt{\frac{Z_{in} \cdot Rs_{ant} \cdot C_{eq}}{L_{ant}}}}{1 - \frac{Z_{in} \cdot Rs_{ant} \cdot C_{eq}}{L_{ant}}} \quad (7)$$

$$\text{with} \quad C_{eq} = \frac{1}{(\omega_0)^2 \cdot L_{ant}} = \frac{C_1 \cdot C_2}{C_1 + C_2} + C_2 \quad (8)$$

REMOTE ACTUATION EXPERIMENT

At the emission, an electronic card is able to provide an AC current till 1A/18V through the transmitter antenna. The card is controlled by a computer that modulates the current amplitude in real time. The receiver antenna is tuned to the operating frequency 13.56 MHz with a discrete capacitor. The induced voltage as a function of distance for two transmitter antennas is reported in figure 11. The signal is then rectified using discrete diodes and capacitors. Remote powering of an array of 128 actuators has been successfully performed. The pull-in voltage was 50 V for beam

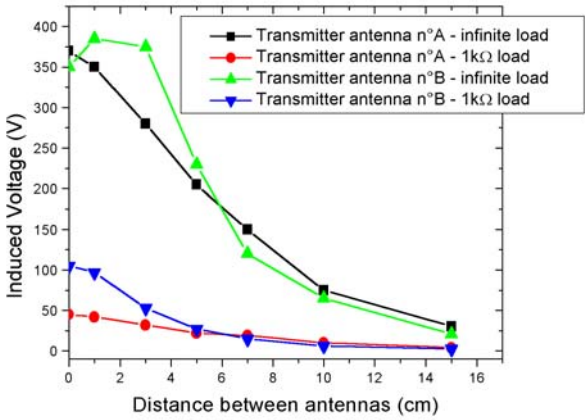

Figure 11: Measured peek to peek induced voltage on antenna n°3 tuned at 13.56 MHz with two transmitter antennas. Antenna A: 2 turns, 14 cm diameter. Antenna B: 4 turns, 7 cm diameter.

thickness reduced to 0.67 µm. Loaded with a 380 µm thick silicon piece of 0.25 mm^2, corresponding approximately to the weight the actuators will have to support once acting as a robot, the pull-in voltage becomes 80 V.

CONCLUSION

A new large stepwise actuator has been successfully telepowered thanks to a gold electroplated antenna processed on an epoxy substrate. A simple analytical model of inductive coupling has been developed in order to optimize the antenna design. These components are ideal for the realization of a completely autonomous microrobot. Future work will consist in the design of a high voltage IC to control such actuators in a Ciliary Motion System.

REFERENCES

[1] M. Ataka, A. Omodaka, N Takeshima and H. Fujita, "Fabrication and operation of polyimide bimorph actuators for a ciliary motion system", *JMEMS*, vol. 2, n°4, dec. 1993, pp. 146-50.

[2] M. Takeda, "Application of MEMS to industrial inspection", *Proceeding of MEMS'01*, pp. 182-91.

[3] T. Ebefors, J. U. Mattsson and E. Kälvesten, "A walking silicon micro robot", *Proceeding of Transducer'99*, pp. 1202-5.

[4] J. A. Von Arx and K. Najafi, "On-chip coils with integrated cores for remote inductive powering of integrated microsystem", *Proceeding of Transducer'97*, pp. 999-1002.

[5] T. Akiyama, D. Collard, and H. Fujita, "Scratch Drive Actuator With Mechanical Links for Self-Assembly of Three-Dimensional MEMS", *JMEMS,* vol. 6, no. 1, Mar. 1997, pp 10-17.

[6] C. P. Yue and S. S. Wong, "On-chip spiral inductors with patterned ground shields for Si-based RF IC's", *JSSC*, vol. 33, n°5, pp. 743-7, may 1998

[7] K. Finkenzeller, *RFID handbook*, John Wiley & son, 1999, p. 68.

[8] T. H. Lee, *The design of CMOS radio frequency integrated Circuit*, Cambridge University Press, 1998, p. 49.